Current density-voltage analyses and interface characterization in Ag/DNA/p-InP structures

Ö. Güllü,[1] O. Pakma,[1,a)] and A. Türüt[2,3]
[1]*Department of Physics, Faculty of Sciences and Arts, Batman University, 72060 Batman, Turkey*
[2]*Department of Physics, Faculty of Sciences and Arts, Atatürk University, 25240 Erzurum, Turkey*
[3]*Department of Physics Engineering, Faculty of Sciences, Istanbul Medeniyet University, 34000 İstanbul, Turkey*

(Received 16 May 2011; accepted 14 January 2012; published online 17 February 2012)

The current density-voltage (J-V) characteristics of Ag/DNA/p-InP metal-insulator-semiconductor (MIS) structures have been investigated in room temperature. We have observed that the Ag/DNA/p-InP structure shows an excellent rectifying behavior and that this structure increases the barrier height (ϕ_{b0}). The main electrical parameters of these structures, such as ideality factor (n), barrier height, and average series resistance values were found to be 1.087, 0.726 eV, and 66.92 Ω. This value of n was attributed to the presence of an interfacial insulator layer at the Ag/p-InP interface and the density of interface states (N_{ss}) localized at the InP/DNA interface. The values of N_{ss} localized at the InP/DNA interface were found at 0.675-E_v in the $1.38 \times 10^{12}\,\mathrm{eV}^{-1}\,\mathrm{cm}^{-2}$. © *2012 American Institute of Physics*. [doi:10.1063/1.3684989]

I. INTRODUCTION

Various non-idealities, such as the formation of an insulator layer at the metal/semiconductor interface, energy distribution profile of interface states at the semiconductor/insulator interface, series resistance and inhomogeneous Schottky barrier heights all have an effect upon the electrical characteristics of metal-insulator-semiconductor (MIS) structures. In MIS structures, metal and semiconductor remain separated by an insulating layer and there is a continuous distribution of surface states at semiconductor/insulator interface.[1,2] Although much has been reported on experimental studies of electrical characteristics parameters, such as the ideality factor (n), barrier height (ϕ_{b0}), series resistance (R_s), and surface states (N_{ss}) in MS and MIS structures, there is still a lack of any satisfactory understanding in all details.[3–9]

As a result of the recent progress in semiconductor technology, indium phosphide (InP) has been brought into light as a material offering potentials to develop optoelectronic and high-speed devices.[10] As a semiconductor material for photovoltaic devices, InP has certain advantages when compared to Si and GaAs.[11,12] It has been acknowledged that similar to silicon, InP as the $A^{III}B^{V}$ compound also usually oxidizes; yet, such native oxides are of poorer quality than SiO_2. When a bulk InP surface is coated by an organic layer, native oxide does not form, resulting in a lower number of surface traps, and this has a negative influence upon the device's electrical and optical performance.

Presenting various electrical and optical properties, organic layers could be used to fabricate molecular electronic devices. With low cost and easy processing opportunity, they can be more advantageous over conventional electronic devices with their new roles. Thus, conventional inorganic devices could be replaced by organic devices as an alternative. Of these organic devices, deoxyribonucleic acid (DNA) is regarded as a good candidate to fabricate organic semiconductor devices such as metal-insulating layer-semiconductor (MIS) diodes and solar cells (see Fig. 1).[13] Recent decades have witnessed an increasing prominence for DNA as the blueprint of life in biophysical chemistry research.[14] The molecular code was elucidated 50 years ago when the genetic code was unraveled, which was a revolution in the field of biotechnology. What was found about DNA and about all the technologies and instruments developed after that helped create totally new industries. In biological terms, it is known that DNA serves to code for functional proteins which express genetic hereditary information. However, a recent discovery has been made that DNA can conduct an electrical current, and thus it has been suggested that the molecule could assume other roles which had not been given to it by nature.[14] DNA is a very promising material for molecular-scale systems with some unique advantages; these include nanometer-scale molecular film, adjustable length, and self-assembly property.[15–18] Electronic device applications require an understanding of the electrical conduction mechanism through DNA molecules, in which charge transport is also associated with DNA radiation damage and repair mechanism in biological terms.[16,19] Through direct electrical conductivity measurements, some recent experimental and theoretical studies revealed conducting behaviors in DNA molecules.[16,20–25] Nevertheless, there is still a debate about the exact charge transport mechanism.[16,26] As shown by some recent studies on their electrical conduction, DNA molecules could act as either semiconductor with nano-size dimensions or non-semiconductor materials (i.e., insulator or metal).[20,21,26–29] Seemingly, a new review argues that DNA is an insulator, or at least a wide bandgap semiconductor with nonlinear current-voltage (I–V) characteristics.[30,31] This opinion is also favored by the measurements conducted by Porath *et al.*[20] and Rakitin *et al.*[32] In their measurements of semiconductor properties for poly(G)–poly(C) molecules, Porath *et al.*[20] used a molecular

a)Electronic mail: osman@pakma.com.

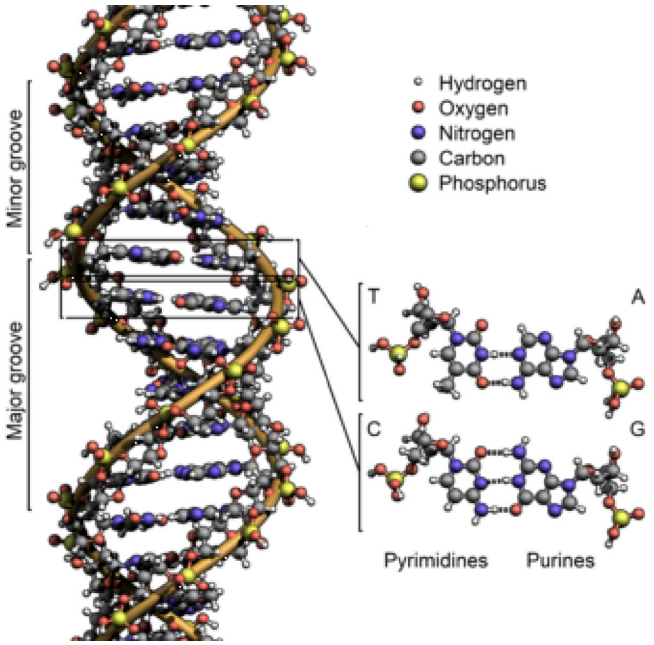

FIG. 1. (Color online) The structure of the DNA double helix (Wikipedia).

band model in which holes move between delocalized electronic states by hopping under bias.[31] Rakitin *et al.*[31] reported metal-like conduction properties in M-DNA and semiconductor-like conduction properties in B-DNA. Yoo *et al.*[22] and Hwang *et al.*[23] also supported these results. Furthermore, Yoo *et al.*[22] reported potential field-effect transistor operation in DNA at room temperature.

Recently, researchers have been highly interested in the possibility to use DNA bases in electronic devices, such as organic field effect transistors and organic/inorganic Schottky structures. Moreover, only tubes of varying proportions are obtained through available techniques. Therefore, there is a need to develop even smaller electronic devices and this is related to the field of DNA electronics. Here, DNA has the possibility to solve many problems since it is the best nanowire available than can self-assemble, self-replicate, and adopt different states and conformations. DNA's most significant property in biomolecular engineering is its self-assembling capacity, through which engineers can fabricate nanostructures with much higher precision than classical silicon-based technologies offer. With a cost of only a few US cents, DNA is also a cheap alternative.[14]

In this study, the energy distribution profile of interface states was obtained from the forward bias current density-voltage (J-V) characteristics by taking into account the series resistance and bias dependence of effective barrier height of the Ag/DNA/p-InP structure. Other main diode parameters, such as ideality factor (n), zero-bias barrier height (ϕ_{b0}), doping concentration (N_A), and depletion layer width (W_D) of Ag/DNA/p-InP structure were also determined at room temperature.

II. EXPERIMENT

The Ag/p-InP and Ag/DNA/p-InP structures were fabricated using one side polished p-type InP wafer with $3.5 \times 10^{17}\,\mathrm{cm}^{-3}$ doping density from capacitance-voltage (C-V) measurements given in Ref. 33. The native oxide on the front surface of p-InP was removed in a HF: H_2O (1: 10) solution and finally the wafer was rinsed in de-ionized (DI) (18 MΩ) water for 30 s. Before forming the organic layer on the p-InP substrate, the ohmic contact was made by evaporating Au-Zn (90%–10%) alloy on the back of the substrate, followed by a temperature treatment at 450 °C for 3 min in N atmosphere.

Miller *et al.* have defined genomic DNA isolation.[34] In their procedure, following the cleaning procedures and ohmic metallization, DNA thin film was directly formed by an addition of 10 μL. The DNA solution with a concentration of 200 μg/ml in water is on the front surface of the p-InP wafer. Then it is evaporated in N atmosphere for 2 days to dry off the solvent. The researchers' preference for the amount of 10 μL DNA solution was based on the results of their tests for various factors which might influence the organic film thickness and homogeneity depending on solution concentration and substrate area. Other factors are also thought to affect organic film quality, including film-forming ability, molecular symmetry, and structure.[33] The thickness of the DNA film on the InP semiconductor was found to be 64.2 nm by using the high-frequency C–V technique ($C = \varepsilon_s A/d$). The top metal dots in contact of the 1.0 mm diameter were formed by evaporating Ag. Furthermore, Ag/p-InP without an organic layer was also produced to make a comparison with the electrical parameters of the Ag/DNA/p-InP device. All evaporation processes were performed in a vacuum coating unit at about 10^{-5} Torr. Figure 2 shows the structure of Ag/DNA/p-InP.

The current-voltage (I-V) measurements were performed using a Keithley 487 Picoammeter/Voltage source. The forward and reverse bias C-V measurements were performed by using an HP 4192 A LF impedance analyzer (5 Hz to 13 MHz) at 1 MHz and with a test signal of 50 $\mathrm{mV_{rms}}$. All measurements were carried out at room temperature and in a dark environment.

III. RESULTS AND DISCUSSION

The current density across ideal SBDs at forward bias voltage, based on the thermionic emission current, is given by the relation[1]

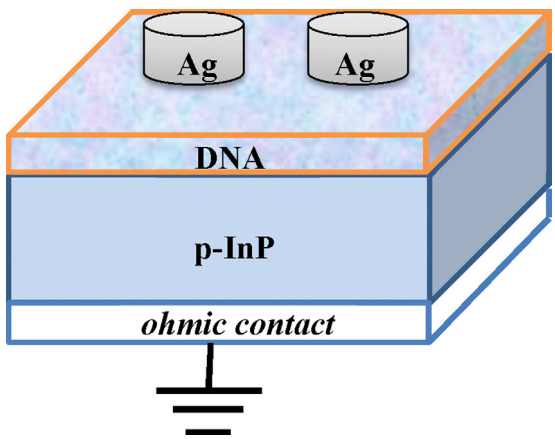

FIG. 2. (Color online) Schematic diagram of the Ag/DNA/p-InP structure.

$$J = J_0 \exp\left(\frac{q(V - JR_S)}{nkT}\right)\left[1 - \exp\left(\frac{-q(V - JR_S)}{kT}\right)\right], \quad (1)$$

where

$$J_0 = A^* T^2 \exp\left(-\frac{q\phi_{b0}}{kT}\right) \quad (2)$$

is the saturation current density, ϕ_{b0} is the zero bias effective barrier height, A^* is the effective Richardson constant (60 A/cm^2 K^2 for p-type InP), n is the ideality factor, q is the electron charge, R_s is the series resistance, and T is the temperature in Kelvin, respectively. It is obtained from the slope of the straight line region of the forward bias ln$J$-V characteristics through the relation

$$n = \frac{q}{kT}\frac{d(V - JR_S)}{d(\ln J)}. \quad (3)$$

Also, the voltage-dependent ideality factor $n(V)$ can be obtained as from Eq. (1),

$$n(V) = \frac{q}{kT}\frac{d(V - JR_S)}{\ln(J/J_0)}. \quad (4)$$

The zero-bias barrier height (ϕ_{b0}) can be obtained from Eq. (2) as

$$\phi_{b0} = \frac{kT}{q}\ln\left(\frac{A^* T^2}{J_0}\right). \quad (5)$$

Figure 3 shows the experimental ln$J$-V characteristics of the reference (Ag/p-InP) and Ag/DNA/p-InP structures at room temperature. As can be seen in Fig. 3, the Ag/DNA/p-InP structure exhibits excellent rectifying behavior. Rectifying interfaces are characterized by weak voltage dependence of reverse-bias current and an exponential increase in forward-bias current. Rapid domination of the current curve in forward bias by series resistance from contact wires or bulk resistance of the organic material and inorganic semiconductor leads to curvature at high current in the ln$J$-V plot. As shown in the figure, a significant decrease occurs in the leakage current of the Ag/DNA/p-InP structure, compared to that of the reference (Ag/p-InP) structure. Since leakage current is inversely proportional to the barrier height, we will deal with this issue and barrier height together below. What is said of the barrier height also applies to the leakage current. The thermionic emission theory with a thin interfacial layer suggests that we can obtain the ideality factor n and barrier height (BH) ϕ_b from the slopes and current axis intercepts of the linear regions in the forward bias J–V plots, respectively. The values of the BH and the ideality factor for the Ag/DNA/p-InP diode have been calculated as 0.726 eV and 1.087, respectively. The ideality factor simply based on the image-force effect should be about 1.01 or 1.02.[35–37] Our results clearly show that the diode's ideality factor significantly exceeds this value.

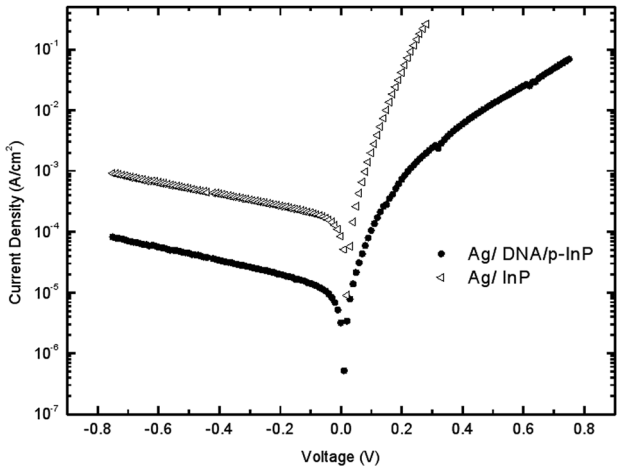

FIG. 3. Forward and reverse bias J-V characteristics of the reference Ag/p-InP and Ag/DNA/p-InP structures at room temperature.

As said before, as determined from the J-V characteristics of the Ag/p-InP reference diode in Fig. 3, the BH value of 0.726 eV for the Ag/DNA/p-InP contact is higher than 0.649 eV. Clearly, the DNA organic thin film formed on the inorganic substrate significantly increased the BH of Schottky diodes, which could be attributed to the fact that an organic interlayer affected the space charge region of the inorganic substrate, thus modifying the effective BH.[38] It is well-known that the organic film acts like a barrier between metal and InP surface. Apparently, despite the abruptness and non-reactivity of the organic/inorganic interface, the DNA organic layer significantly modified the interface states.[38–40]

In our previous study, we modified the DNA organic layer with Al metal and examined the current-voltage characteristics of Al/DNA/p-InP structures at room temperature.[41] From the current-voltage characteristics of Al/DNA/p-InP structure at room temperature, we had computed the diode ideality factor and barrier height as 1.26 and 0.96 eV, respectively.[41] In our present study, the ideality factor value for Ag/DNA/p-InP structure is clearly closer to ideality when compared to that of Al/DNA/p-InP structure. Furthermore, the barrier height was found to be lower. A qualitative interpretation suggested for the change in barrier height is an interface dipole as a result of organic layer passivation.[38,39,42,43] An important aspect for metal-on organic interfaces is the work function of the evaporated metal, which strongly depends on the crystalline structure and morphology of the film.[43] Zahn *et al.* argue that there is a correlation between the initial decrease or increase observed in an organic interlayer's effective barrier height and the energy level aligned between the lowest unoccupied molecular orbital (LUMO) and the conduction band minimum (CBM) of the inorganic semiconductor at the organic/inorganic semiconductor interface.[44]

It is seen as a downward concave curvature at the forward bias current density-voltage plot for sufficiently large voltages in Fig. 3. In the organic/inorganic structures, it is well known that the soled "downward concave curvature" of current density for forward values of bias may be assigned to the occurrence of the Fowler-Nordheim (FN) effect. Our device with the Ag cathode shows that the carrier injection limitation is located at the organic/cathode interface and the

FN mechanism is qualitatively consistent with experimental data at high voltages. Therefore, a different mechanism apart from thermionic emission seems to become dominant to limit the current at high voltages. Figure 4 shows the *J-V* data in the ln(*J*/*V*) versus 1/*V* plot to see if it fits with the FN tunneling formula,[45]

$$J\alpha F^2 e^{-\kappa/F}, \tag{6}$$

where $F = V/d$ is the electric field strength and κ is a parameter that depends on the barrier shape. Assuming the injected charge is tunneling through a triangular barrier the constant κ in Eq. (5) is given by

$$\kappa = 8\pi(2m^*)^{1/2}\varphi^{3/2}/3qh, \tag{7}$$

where φ is the Schottky energy barrier, m^* the effective mass of the charge carriers, q the magnitude of the electronic charge, and h is Planck's constant.[44] In the process of injection, if the device obeys the FN tunneling mechanism, the log of current will exhibit a linear relationship with the reciprocal value of the field. It can be seen that the *J-V* data in the Fig. 4 fit very well with the FN tunneling formula in a wide range of the current at high voltages for the device. From the slope of the straight line, the injection barrier height for carriers is estimated. The barrier height was calculated as 0.69 eV for the device. Our result is in good agreement with that obtained from Eq. (6).

The series resistance (R_s) is an important parameter particularly in the downward curvature of the forward bias *J-V* characteristics at a sufficiently high bias voltage. Both the R_s in the structure and resistance of the epitaxial layer could be the reason why the characteristics deviated from linearity in higher forward biases.[46,47] In this case, to determine the ϕ_{b0} and R_s, Norde's function method can be used.[48] The Norde's function are given as

$$F(V) = \frac{V}{\gamma} - \frac{kT}{q}\ln\left(\frac{J(V)}{A^*T^2}\right), \tag{8}$$

where γ is an dimensionless integer greater than n. Once the minimum of the F versus V plot is determined, the value BH can be obtained from Eq. (9), where $F(V_0)$ is the minimum point of $F(V)$, and V_0 is the corresponding voltage,

$$\phi_0 = F(V_0) + \frac{V_0}{\gamma} - \frac{kT}{q}. \tag{9}$$

R_s values are determined as

$$R_S = \frac{kT(\gamma - n)}{qJ}. \tag{10}$$

Figure 5 shows $F(V)$-V plots of the Ag/*p*-InP and Ag/DNA/*p*-InP diodes. From the $F(V)$-V plots, some parameters of the diodes (ϕ_{b0}, R_s) are determined and they are shown in Table I. As demonstrated by the high R_s value, R_s limits the current in this structure. Series resistance has an effect similar to that of the series combination of a diode and a resistance R_s. To express the voltage passing across the diode, we use the total voltage drop across the diode and the resistance R_s. A very high R_s value could be due to a decrease in the exponentially increasing current rate as a result of a space-charge injection into OG thin film at higher forward bias voltage.

In the downward curvature of the forward bias *J-V* characteristics, R_s seems to stand out, while all of the forward bias region is affected by interface states (N_{ss}), whose distribution varies from one region to another in the bandgap at the semiconductor/insulator interface. Considering the bias dependence of the ideality factor, barrier height, and series resistance, the forward bias *J-V* characteristics could give the energy density distribution profile of these N_{ss} for Ag/*p*-InP and Ag/DNA/*p*-InP diodes. Since there is an interfacial insulator layer and interface states at the InP/DNA interface, we assume that effective barrier height (ϕ_e) depends on bias voltage. Voltage- and series-resistance-dependent effective barrier height is expressed as follows:[49–51]

$$\phi_e = \phi_{b0} + \beta(V - JR_S) = \phi_{b0} + \left(1 - \frac{1}{n(V)}\right)(V - JR_S), \tag{11}$$

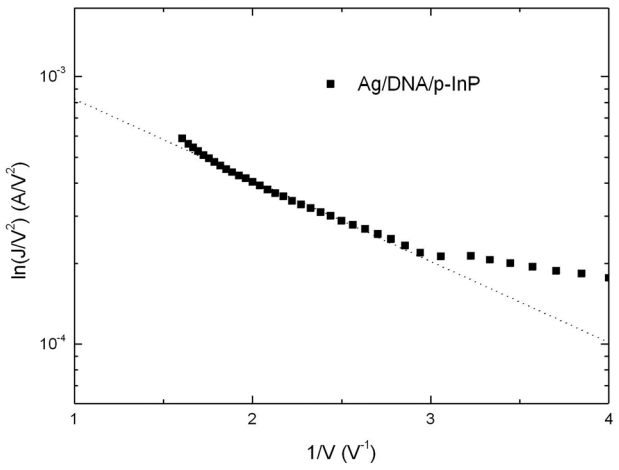

FIG. 4. Fowler-Nordheim (FN) plot of the Ag/DNA/*p*-InP structure at forward bias.

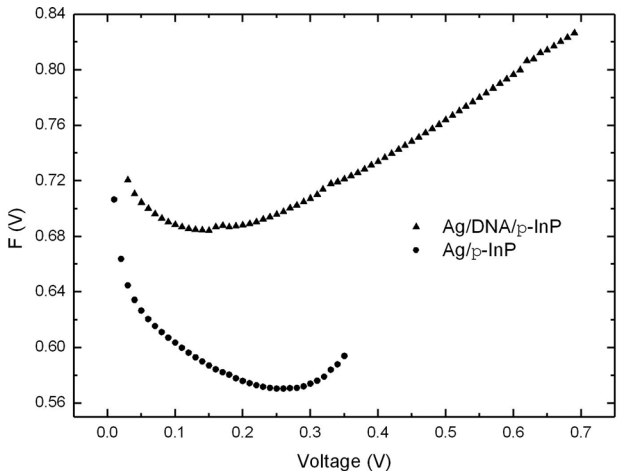

FIG. 5. $F(V)$ vs V plot of the Ag/*p*-InP and Ag/DNA/*p*-InP structures.

TABLE I. Various parameters determined from the forward bias J-V characteristics of Ag/p-InP and Ag/DNA/p-InP diodes.

Sample	n	ϕ_{b0} (eV)	R_s (Ω)	ϕ_{b0} (eV) [F(V)-V]
Ag/*p*-InP	1.03	0.649	14.84	0.674
Ag/DNA/*p*-InP	1.087	0.726	66.92	0.794

where β is used in place of the zero bias barrier height (ϕ_{b0}) as the voltage coefficient of the effective barrier height. This parameter covers the effect of both interface states in equilibrium with semiconductor. As for the Ag/p-InP and Ag/DNA/p-InP diodes, Card and Rhoderick's expression of the density of interface states, which could be reduced as follows:[2,3]

$$N_{ss}(V) = \frac{1}{q}\left[\frac{\varepsilon_i}{\delta}(n(V)-1) - \frac{\varepsilon_s}{W_D}\right], \tag{12}$$

where δ is the thickness of the interfacial insulator layer, W_D is space charge width, and ε_0 is the permittivity of free space. As for p-type semiconductors, we could write the following equation for the energy of interface states E_{ss} with respect to the bottom of valance band at the semiconductor surface:[3]

$$E_{ss} - E_v = q(\phi_e - V). \tag{13}$$

In the ideal case, the depletion layer capacitance of Ag/DNA/p-InP diodes per unit area can be expressed as[1]

$$C^{-2} = \frac{2(V_d + V)}{\varepsilon_0 \varepsilon_s q A^2 N_A}, \tag{14}$$

where V_d is the diffusion potential at zero bias and N_A is acceptor concentration. The C^{-2}-V plot of the Ag/DNA/p-InP diode is given in Fig. 6 at 500 kHz. The acceptor doping density N_A was obtained from the slope of C^{-2}-V plot, while the depletion layer width was calculated from C-V measurements using the following equation:

$$W_D = \sqrt{\frac{2\varepsilon_s V_d}{qN_A}}. \tag{15}$$

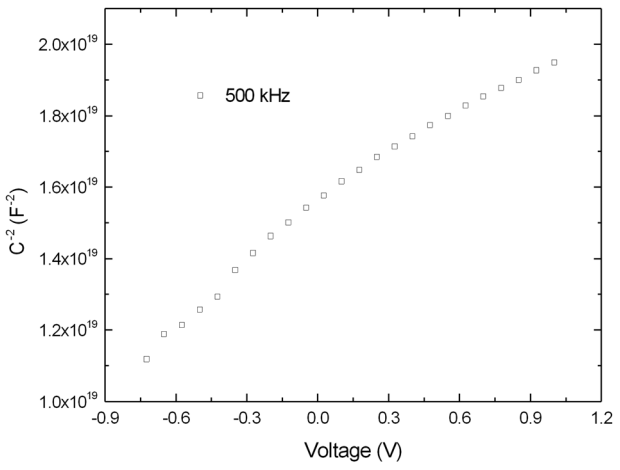

FIG. 6. The energy distribution profile of interface states of the Ag/DNA/p-InP structure at room temperature.

As shown in Fig. 6, Eq. (12) was used to obtain the energy distribution profile of interface states N_{ss} for Ag/p-InP and Ag/DNA/p-InP diodes when R_s values from the experimental forward bias J-V characteristics are considered. As is clear from the same figure, there is an obvious increase in interface states values from mid gap toward the top of valance band. The values of N_{ss} localized at the InP/DNA interface were found at 0.675-E_v in the $1.38 \times 10^{12}\,\mathrm{eV}^{-1}\,\mathrm{cm}^{-2}$.

IV. CONCLUSION

The current density-voltage (J-V) characteristics of Ag/DNA/p-InP MIS structures have been investigated at room temperature. The main electrical parameters of these structures, such as ideality factor (n), barrier height and average series resistance values were found to be 1.087, 0.726 eV, and 66.92 Ω. The value of ideality factor can be attributed to the presence of a wide distribution of low Schottky barrier height patches, insulator layer (DNA), the particular distribution of interface states (N_{ss}) at the InP/DNA interface, and the series resistance of structure. The values of N_{ss} localized at the InP/DNA interface were found at 0.675-E_v in the $1.38 \times 10^{12}\,\mathrm{eV}^{-1}\,\mathrm{cm}^{-2}$.

[1]S. M. Sze and K. Ng Kwok, *Physics of Semiconductor Devices*, 3rd ed. (John Wiley, New Jersey, 2007).
[2]E. H. Rhoderick and R. H. Williams, *Metal-Semiconductor Contacts*, 2nd ed. (Clarendon Press, Oxford, 1978).
[3]H. C. Card and E. H. Rhoderick, J. Phys. D **4**, 1589 (1971).
[4]O. Pakma, N. Serin, T. Serin, and S. Altindal, J. Appl. Phys. **104**, 014501 (2008).
[5]A. Singh, K. C. Reinhardt, and W. A. Anderson, J. Appl. Phys. **68**, 3478 (1990).
[6]S. Karatas, S. Altindal, A. Turut, and A. Ozmen, Appl. Surf. Sci. **252**, 1732 (2005).
[7]A. S. Kavasoglu, F. Yakuphanoglu, N. Kavasoglu, O. Pakma, O. Birgi, and S. Oktik, J. Alloy. Compd. **492**, 421 (2010).
[8]S. Pandey and S. Kal, Solid State Electron. **42**, 943 (1998).
[9]P. Chattopadhyay and B. Raychaudhuri, Solid-State Electron. **36**, 605 (1993).
[10]K. Hattori and Y. Torii, Solid-State Electron. **34**, 527 (1991).
[11]D. P. Halliday, M. D. G. Potter, and K. Durose, *IOP Meeting on Thin Film Photovoltaic Materials and Devices*, London, Sept. 2001.
[12]P. Nollet, M. Burgelman, S. Degrave, and M. Kontges, in *Proceedings of the 29th IEEE Photovoltaic Specialists Conference* (PVSC, Piscataway, USA, 2002).
[13]O. Gullu and A. Turut, Sol. Energy Mater. Sol. Cells **92**, 1205 (2008).
[14]V. Bhalla, R. P. Bajpai, and L. M. Bharadwaj, EMBO Rep. **4**, 442 (2003).
[15]J. S. Hwang, S. H. Hong, H. K. Kim, Y. W. Kwon, J. I. Jin, S. W. Hwang, and D. Ahn, *Extended Abstracts of the 2004 International Conference on Solid State Devices and Materials* (SSDM, Tokyo, 2004).
[16]J. S. Hwang, S. W. Hwang, and D. Ahn, Superlattices Microstruct. **4**, 433 (2003).
[17]O. Gullu, M. Cankaya, O. Baris, M. Biber, H. Ozdemir, M. Gulluce, and A. Turut, Appl. Surf. Sci. **254**, 5175 (2008).
[18]C. A. Mirkin, R. L. Letsinger, R. C. Mucic, and J. J. Storhoff, Nature **382**, 607 (1996).
[19]P. J. Dandliker, R. E. Holmlin, and J. K. Barton, Science **275**, 1465 (1997).
[20]D. Porath, A. Bezryadin, S. deVries, and C. Dekker, Nature **403**, 635 (2000).
[21]A. Y. Kasumov, M. Kociak, S. Gueron, B. Reulet, V. T. Volkov, D. V. Klinov, and H. Bouchiat, Science **291**, 280 (2001).
[22]K. H. Yoo, D. H. Ha, J. O. Lee, J. W. Park, J. Kim, J. J. Kim, H. Y. Lee, T. Kawai, and H. Y. Choi, Phys. Rev. Lett. **87**, 198102 (2001).
[23]J. S. Hwang, K. J. Kong, D. Ahn, G. S. Lee, D. J. Ahn, and S. W. Hwang, Appl. Phys. Lett. **81**, 1134 (2002).
[24]X. Q. Li and Y. J. Yan, Appl. Phys. Lett. **79**, 2190 (2001).

[25]G. Cuniberti, L. Craco, D. Porath, and C. Dekker, Phys. Rev. B **65**, 241314 (2002).
[26]A. J. Storm, J. Van Noort, S. de Vries, and C. Dekker, Appl. Phys. Lett. **79**, 3881 (2001).
[27]L. Cai, H. Tabata, and T. Kawai, Appl. Phys. Lett. **77**, 3105 (2000).
[28]H. W. Fink and C. Schonenberger, Nature **398**, 407 (1999).
[29]Y. S. Jo, Y. Lee, and Y. Roh, Mater. Sci. Eng., C **23**, 841 (2003).
[30]R. G. Endres, D. L. Cox, and R. R. P. Singh, Rev. Mod. Phys. **76**, 195 (2004).
[31]H. L. Kwok, IEE Proc.: Nanobiotechnol. **151**, 193 (2004).
[32]A. Rakitin, P. Aich, C. Papadopoulos, Y. Kobzar, A. S. Wedeneev, J. S. Lee, and J. M. Xu, Phys. Rev. Lett. **86**, 3670 (2001).
[33]O. Gullu, A. Turut, and S. Asubay, J. Phys.: Condens. Matter **20**, 045215 (2008).
[34]A. Miller, D. D. Dykes, and H. F. Polesky, Nucleic Acids Res. **16**, 1215 (1988).
[35]R. T. Tung, Phys. Rev. B **45**, 13509 (1992).
[36]W. Monch, J. Vac. Sci. Technol. B **17**, 1867 (1999).
[37]R. F. Schmitsdorf, T. U. Kampen, and W. Monch, J. Vac. Sci. Technol. B **15**, 1221 (1997).
[38]A. R. V. Roberts and D. A. Evans, Appl. Phys. Lett. **86**, 072105 (2005).
[39]T. U. Kampen, S. Park, and D. R. T. Zahn, Appl. Surf. Sci. **190**, 461 (2002).
[40]S. R. Forrest, M. L. Kaplan, and P. H. Schmidt, J. Appl. Phys. **60**, 2406 (1986).
[41]O. Gullu, M. Cankaya, O. Baris, and A. Turut, Microelectron. Eng. **85**, 2250 (2008).
[42]T. U. Kampen, A. Schuller, D.R.T. Zahn, B. Biel, J. Ortega, R. Perez, and F. Flores, Appl. Surf. Sci. **234**, 341 (2004).
[43]T. U. Kampen, A. Das, S. Park, W. Hoyer, and D. R. T. Zahn, Appl. Surf. Sci. **234**, 333 (2004).
[44]D. R. T. Zahn, T. U. Kampen, and H. Mendez, Appl. Surf. Sci. **212–213**, 423 (2003).
[45]S. Y. Park, C. H. Lee, W. J. Song, and C. Seoul, Curr. Appl. Phys. **1**, 116 (2001).
[46]J. P. Sullivan, R. T. Tung, M. R. Pinto, and W. R. Graham, J. Appl. Phys. **70**, 7403 (1991).
[47]S. Chand and J. Kumar, Semicond. Sci. Technol. **11**, 1203 (1996).
[48]H. Norde, J. Appl. Phys. **50**, 5052 (1979).
[49]E. H. Nicollian and J. R. Brews, *Metal-Oxide Semiconductor (MOS) Physics and Technology* (Wiley, New York, 1982).
[50]M. K. Hudait and S. B. Krupanidhi, Mater. Sci. Eng., B **87**, 141 (2001).
[51]M. K. Hudait, P. Venkateswarlu, and S. B. Krupanidhi, Solid-State Electron. **45**, 1332 (2001).